

Establishing Controlled Source MT at GFZ

M. Becken^{1,2}, R. Streich^{1,2}, O. Ritter²

1 Potsdam University, Department of Geosciences, Karl-Liebknecht-Strasse 24, 14476 Potsdam, Germany

2 Helmholtz Centre Potsdam GFZ German Research Centre for Geosciences, Telegrafenberg, 14473 Potsdam, Germany

Summary

The multidisciplinary GeoEn project (the Brandenburg pilot project in the BMBF program „Spitzenforschung und Innovation in den Neuen Ländern“) integrates research in the fields of geothermal energy, carbon dioxide capture, transport and storage (CCTS) as well as the exploration of unconventional gas reserves (shale gas). The electrical conductivity is one key parameter to characterize reservoirs and to monitor changes due to circulation or injection of fluids at reservoir depth. Bulk electrical conductivity is highly sensitive to fluids within interconnected pores, and therefore EM techniques are powerful tools for exploring and monitoring geothermal reservoirs, CO₂ storage sites and shale gas reservoirs. In the framework of the GeoEn project, we establish Controlled Source MT (CSMT) at GFZ Potsdam. We aim at combining active and passive MT to image the electrical conductivity structure within the Earth, ultimately in 3D.

For CSMT, we intend to use grounded electrodes to inject a frequency-dependent current into the Earth and measure the induced electric and magnetic fields at near-field to far-field distances. We will use novel transmitter systems from Metronix (Braunschweig) which are presently under development. Standard MT receivers will be utilized to measure the induced electric and magnetic fields. In the scope of the project, we will (i) assemble the transmitter system and the source dipole, (ii) optimize and design CSMT field procedures for geothermal exploration, carbon dioxide reservoir characterization and shale gas exploration (Streich et al., 2010a), (iii) develop and implement time-series processing, (iv) develop and implement 1D modeling (Streich and Becken, 2009) and inversion software and 3D modeling codes (Streich, 2009; Streich et al., 2010b).

In this contribution, we describe a test of long steel electrodes as the current electrodes of the source dipole, and we examine the resolution power of CSMT using 1D inversion of synthetic data.

Current electrodes of CSMT source dipole

Low grounding resistances of the current electrodes are crucial for injecting strong currents into the subsurface. The Metronix 22 kVA transmitter generates currents of max. 40 A (560 V), which can, however, only be achieved if the total resistance of the dipole (1-km long cable and grounding electrodes) is less than 14Ω. We use a thick cable that has a resistance of 2Ω/km. Accordingly, to achieve maximum currents, the electrode grounding resistances should be less than 12Ω. At high frequencies, the maximum current will be further limited by the inductance of the cable.

The grounding resistance depends primarily on the surface of the electrode that is in contact with the ground, and the surrounding resistivity within the Earth. For a homogenous earth, the grounding resistance R of a steel rod is

$$R = \frac{\rho}{2\pi L} \ln \left(\frac{4L}{a} - 1 \right), \quad (1)$$

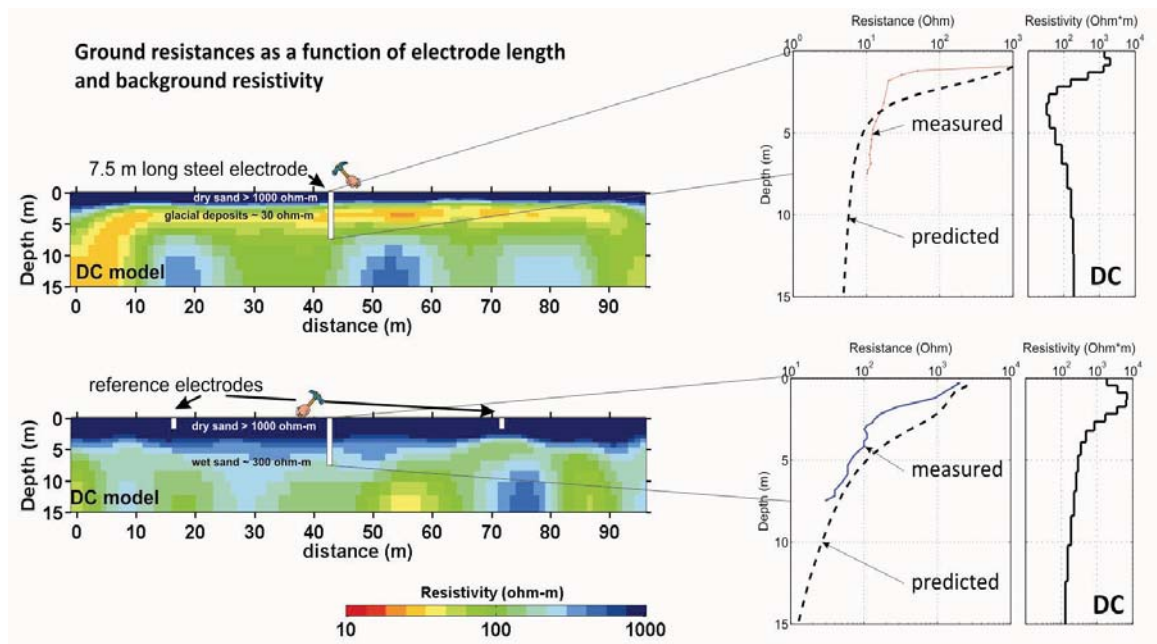


Figure 1: Electrode test. We measured the ground resistance of a steel electrode (diameter 32 mm) vs. depth of the rod at two different locations, which may represent typical conditions in northern Germany. Ground resistance measurements were taken against two reference electrodes at ~30 m distance to the left and right. DC Wenner spreads were measured at the same locations (left panels). The panels to the right show the measured resistances (red and blue lines), compared to theoretical predictions (dashed black lines) based on the resistivity-depth profiles at the electrode locations shown in the rightmost plots. The sudden drop in resistance at <2m depth is mainly attributed to the penetration of the groundwater table. Further resistance reduction is due to increased surface of the electrode with increased penetration depth.

where L is the length of the rod in the ground, a is the diameter, and ρ is the earth resistivity. Note that the resistance decreases slowly for increasingly large electrode lengths L . In practice, we plan to use up to 15-m long steel electrodes with $a = 3.2$ cm, which would result in a grounding resistance

$$R \approx \frac{\rho}{12.5 m} (\Omega), \quad (2)$$

assuming homogeneous ground resistivity. This suggests that $\rho < 75 \Omega\text{m}$ would represent suitable conditions at the grounding point to achieve sufficiently small resistances $R < 6 \Omega$ with 15 m long electrodes. However, we hope that the steel rods penetrate conductive material at shallower depth (e.g. groundwater), which would further reduce the resistance or the required electrode length.

We have tested the grounding resistance of long steel electrodes in a geoelectrically known environment near Nauen, Germany (Figure 1). We rammed two electrodes into the ground and measured the resistances every ~0.3 m against two 2-m long reference electrodes. As expected, the resistances were observed to decrease with increasing penetration depth, starting at >3 k Ω at <1m and decaying approximately exponentially with depth. At ~7.5 m depth, we achieved ~10 Ω at one test location (upper panels in Figure 1), and ~30 Ω at the other test location (lower panels).

The approximate subsurface resistivities at the test locations were determined from 2D DC resistivity sections. At both sites, high resistivities within the upper 2-3 m correspond to a dry sand layer. At

greater depths, we penetrate conductive glacial till at test location 1 (upper panel in Figure 1) and a groundwater layer at test location 2 (lower panel). The measured grounding resistance values are roughly consistent with predictions (dashed lines) based on the geometry and the subsurface resistivity distribution. For resistance predictions, we approximated the resistance R from a parallel circuit of steel rod segments of length ∂L embedded into a medium with piecewise constant resistivity ρ_i . Approximate ρ_i values were extracted from the 2D DC resistivity-depth sections. Let the individual rod pieces have resistance

$$R_i = \frac{\rho_i}{2\pi\partial L} \ln\left(\frac{4\partial L}{a} - 1\right), \quad (3)$$

then the resistance of the entire rod to a depth L is given by

$$\frac{1}{R} = \sum_i \frac{1}{R_i}. \quad (4)$$

Equations 3 and 4 were used to estimate grounding resistances from the 2D resistivity models (Figure 1).

This test shows that long steel rods may be suitable electrodes for CSMT source dipoles. At one test location with favorable geology (glacial till), we achieved a ground resistance of $\sim 10 \Omega$ with electrodes penetrating 7.5 m deep; the second test location, a sandy soil with a freshwater layer at ~ 3 m depth, may require deeper electrodes. Our predictions suggest that the ground resistance of the steel rod may drop at this location to values of $\sim 10 \Omega$ at ~ 15 m depth. The simple model used to predict grounding resistance has proven to be useful for practical purposes. Before installing electrodes, it may be advisable to investigate potential locations with DC resistivity soundings in order to predict expectable resistances and required electrode lengths.

1D CSMT Inversion

Vertical currents, galvanically injected into the subsurface with a grounded dipole source, exhibit sensitivity to buried resistors at depth. This makes the CSMT technique suitable for imaging resistive layers, whereas both passive MT and CSMT are sensitive to conductive layers. The effect of anomalously resistive subsurface structures on surface CSMT data is typically smaller in land applications than in deep-water marine applications. Land applications of frequency-domain CSMT suffer from energy travelling through the air even more than marine applications, which obscures the response from deeper targets. Nevertheless, forward modeling studies suggest that in many cases, the e.m. response of thin resistive layers is above noise level (see Streich and Becken, this issue).

A practical question is to what extent the resistivity models giving rise to these anomalies can be recovered from measured data. We ran 1D Occam-type inversions to investigate the resolution power of CSMT data. To infer the resistivity structure from 1D inversion, we can exploit the spatial decay of CSMT fields with increasing distance to the source, and the frequency dependency of the fields. In land-based applications, we will typically have only few source locations combined with a relatively large number of receivers (say, 100), and potentially long transmitting times that allow us to cover a broad frequency range. In contrast, marine applications use a source towed continuously over a number of receivers, effectively yielding many source point locations, but only short transmitting times and thus a narrow frequency band for a given source location. Hence, land applications will primarily utilize the frequency

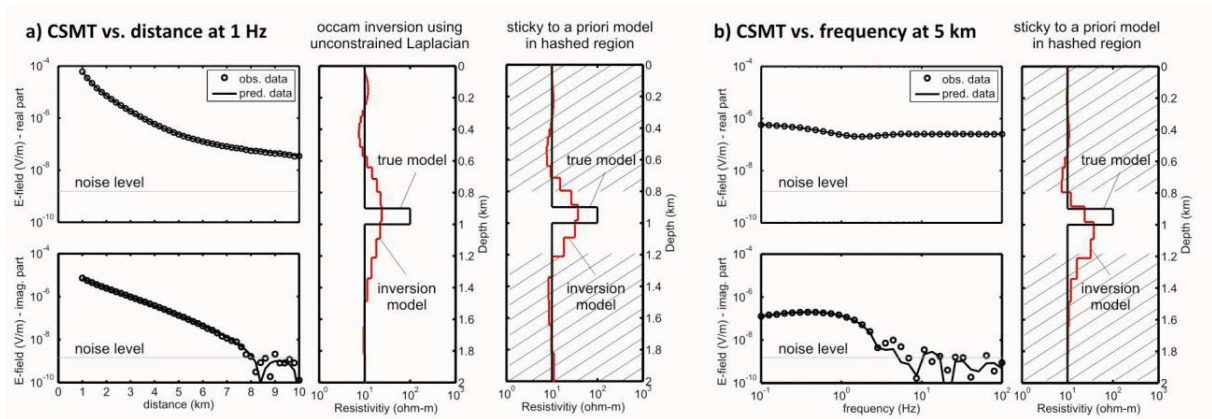


Figure 2: 1D Occam inversion of synthetic CSMT data. The data are the real and imaginary parts of the inline electric field, contaminated with white noise with 1% of the signal amplitude. In addition, white noise with a standard deviation of 10^{-9} V/m was added. **a)** Inversion of the spatial decay of the field for a single frequency (1 Hz), using an unconstrained Occam inversion and using an Occam variant where the deviation from an a priori model is penalized outside of the depth of interest. **b)** Inversion of the frequency spectrum recorded at 5 km distance from the transmitter.

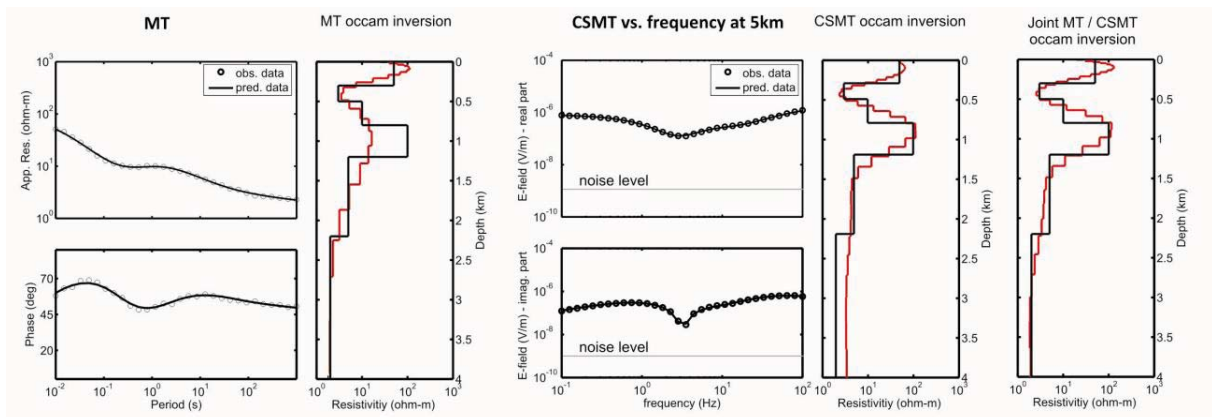


Figure 3: Comparison of single and joint 1D inversion models for passive MT and CSMT data. In (a), the left panel shows passive MT data (apparent resistivity and phase) for the true model and MT inversion result displayed in the right panel. In (b), CSMT data (real and imaginary part of the inline electric field) are displayed for the true resistivity model and CSMT inversion result. (c) shows the resistivity model resulting from joint MT and CSMT inversion. In this example, the MT data add information only at greater depths, where the sensitivity of CSMT sounding is low. In practice, we anticipate that MT data will help construct a (2D/3D) regional background model, and CSMT data will help refine the model at reservoir scale (1D/3D).

dependency of the fields, whereas marine applications will primarily exploit spatial variations of the fields.

We have implemented a 1D CSMT inversion based on Weidelt's formulation of the forward problem (Weidelt, 2007), and analytically derived expressions for the Jacobian matrix required in the inversion. Finite source dipoles (Streich and Becken, this issue) have been incorporated into the inversion; however, in the present form of the inversion scheme, the source and receivers are placed at the surface. Here, we only consider horizontal electric point dipole sources. The inversion is similar to

Occam inversion (Constable et al., 1987); however, Occam's second phase (i.e., the determination of the regularization parameter that yields optimal trade-off between data residuals and model norm) has not been implemented. Instead, we fix the regularization parameter for one entire inversion run.

Using this inversion scheme, we found that both the inversion of multi-offset data at a single frequency and multi-frequency data at a single receiver location have the power to yield comparable inversion models, if the frequency range and the distance to the transmitter are appropriate for imaging the target depth (Figure 2). The left panels in Figure 2a and b depict the inline electric field as a function of distance from the transmitter for the frequency $f = 1$ Hz and as a function of frequency at 5 km distance, respectively, for a model containing a resistive layer embedded into a homogeneous half-space. Random noise of 1% of the field amplitudes and a noise floor of 10^{-9} V/m were added to the data prior to inversion. The central panel in Figure 2a shows the inversion model obtained from smooth inversion using a standard Laplacian penalty on the logarithmic model resistivities (red line). A similar result (not shown) was obtained from inversion of the multi-frequency electric field data shown in Figure 2b. In both cases, the recovered 1D model contains a resistive zone that is smeared over a wide depth range, because regularization penalizes thin model layers.

For monitoring applications (e.g., CO₂ injection), the depth of interest is known. A focused inversion that searches for deviations from an a priori model primarily at reservoir depth may help improve the model. We have therefore incorporated a term into the Occam inversion that allows us to weight the penalty depending on the difference of every inversion model parameter to an a priori model (Key, 2009). The right panels in Figure 2a and b show the result of this variant of regularized inversion. The hashed areas correspond to depth levels where the inversion model is constrained to deviate minimally from the a priori model (which is the true model in this case), whereas the rest of the model was permitted to vary freely (in the sense of a Laplacian regularization). This approach clearly helps focusing the resistive anomaly at the true depth and may thus be adequate for a focused model search.

The penetration depth of CSMT data is limited by the lowest frequencies used and the greatest offsets providing reasonable signal quality. Combining CSMT with passive MT may prove helpful to expand the model scale. Furthermore, both techniques exhibit different sensitivities to resistive and conductive structures (and to deviations from 1D media) and thus provide complementary information. We have therefore implemented a joint 1D inversion for both data types. In Figure 3, we compare the 1D inversion models for a multi-layered structure obtained from MT data and CSMT data alone and from joint CSMT and MT inversion. Here, the CSMT data are the frequency-dependent inline electric field data, measured at 5 km offset from the transmitter. The individual inversion models show that (i) both techniques resolve shallow conductive layers, (ii) the CSMT data resolve a resistive layer at 1 km depth, and (iii) the MT data resolve the conductivity of the basal layer that is too deep to be sensed with CSMT. All of these model features are revealed by joint inversion, suggesting increased resolution capabilities from combined applications of both techniques.

Acknowledgements

This work is funded by the German Federal Ministry of Education and Research (BMBF) within the framework of the GeoEn project. S. Costabel, TU Berlin, made the DC measurements and provided the 2D inversion models.

References:

Constable, S. C., Parker, R. L. and Constable, C. G., 1987, Occam's inversion: A practical algorithm for generating smooth models from electromagnetic sounding data, *Geophysics* 75(3), 289-300.

Key, K., 2009, 1D inversion of multicomponent, multifrequency marine CSEM data: Methodology and synthetic studies for resolving thin resistive layers, *Geophysics* 74(2), F9-F20.

Streich, R., 2009, 3D finite-difference frequency-domain modeling of controlled-source electromagnetic data: direct solution and optimization for high accuracy, *Geophysics* 74(5), F95-F105.

Streich, R., Becken, M. and Ritter, O., 2010a, Imaging of CO₂ storage sites, geothermal reservoirs, and gas shales using controlled-source magnetotellurics: modeling studies, *Chemie der Erde*, submitted.

Streich, R. and Becken, M., 2010, EM fields generated by finite-length wire sources in 1D media: comparison with point dipole solutions, *Protokoll zum Kolloquium "Elektromagnetische Tiefenforschung"*, Seddiner See, 28.09.-02.10.2009.

Streich, R., Schwarzbach, C., Becken, M. and Spitzer, K., 2010b, Controlled-source electromagnetic modelling studies: utility of auxiliary potentials for low-frequency stabilization, *EAGE 70th Conference and Exhibition*, Barcelona, Spain, submitted.

Weidelt, P., 2007, Guided waves in marine CSEM: *Geophysical Journal International*, 171, 153–176.